Variational calculation for maximal heat transport due to the ion-temperature gradient

Chang-Bae Kim
Physics Department, Soong Sil University, Seoul, Korea 156-743
(Received 22 July 1996)

Variational principle for the maximal heat transport due to turbulence driven by the ion-temperature gradient is studied. Plasma is modeled as a fluid in the slab geometry and energy conservation is enforced for the resulting optimal state. Bounding curve and the profiles of the fluctuations are plotted. Bounds are argued to be, in a limited fashion, of the same order as the true values. [S1063-651X(97)11502-1]

PACS number(s): 52.25.Fi, 52.35.Ra, 52.35.Qz, 52.55.Dy

I. INTRODUCTION

One of the outstanding problems in fusion experiments is the presence of the anomalous transport of the plasma energy. Much effort has been put into characterizing sources of the enhanced transport and of figuring out how to suppress them. An ion-temperature gradient (ITG) [1–3] has been suspected as a prime cause of driving the turbulence because the enhanced confinement is achieved with peaked density profiles [4,5]. Many theoretical and computational works have been devoted to investigating the stability criteria and the turbulent transport resulting from the η_i instability. [6–9] Either one models the plasma as two fluids with the Landau damping simulated one way or another [10] or, if one wants a more sophisticated approach, one adopts the kinetic model of the plasma. Computationally, with the advent of the so-called δf algorithm, the numerical simulations are performed with relatively low noise and parallel processing makes it possible to run with the parameters, which are close to the experimental values. In the current work, though, we do not report the result of the numerical simulation of the model equations. Rather, the result of an approach is presented, which is somewhat different from the existing works: an upper bound for the turbulent heat flux in the steady state is computed via the variational principle that incorporates the physical constraint of the energy conservation. It may not be the real solution of the plasma dynamics if the state of maximal heat transport is not the true state. However, it certainly provides a useful means in predicing the level of the transport and serves as a benchmark. The method, which is often called optimum theory [11], has been successfully applied to many problems in neutral fluids [12] and the plasmas, such as the heat and the momentum transport, passive advection, and magnetic-field reversal [13–15]. In those problems, upper bounds are found to be reasonably close to the true values, even when the energy conservation is the only constraint that is considered. Since, in tokamak experiments, prevailing physics are different in many regions, it is difficult to encompass all the important physics in constraints. In this work, a slice inside the tokamak is cut and the variational principle of local turbulent transport due to ITG is formulated. In this paper we introduce the model equations for the ITG turbulence and formulate the variational principle. The resulting Euler-Lagrange equations are also derived. The bounding curve of the heat flux in terms of η_i and the eigenfunctions are also presented and we summarize the result.

The model fluid equations to be used in the work are [16]

$$0=\frac{\partial}{\partial t}(\phi-\nabla_\perp^2\psi)+\frac{\partial\phi}{\partial y}+\nabla_\parallel u+\mu_\perp\nabla_\perp^4\psi - \nabla_\perp\cdot[\boldsymbol{b}\cdot(\nabla\phi\times\nabla)\nabla\psi], \tag{1}$$

$$0=\frac{\partial u}{\partial t}+\nabla_\parallel\psi+\boldsymbol{b}\cdot(\nabla\phi\times\nabla u)-\nu_\perp\nabla_\perp^2 u-\nu_\parallel\nabla_\parallel^2 u, \tag{2}$$

$$0=\frac{\partial}{\partial t}(p-\tau\Gamma\phi)+\tau\overline{K}\frac{\partial\phi}{\partial y}-\chi_\perp\nabla_\perp^2 p - \chi_\parallel\nabla_\parallel^2 p+\boldsymbol{b}\cdot(\nabla\phi\times\nabla p). \tag{3}$$

In Eqs. (1)–(3), the electric potential, the fluid velocity along the field lines, and the plasma pressure are denoted as ϕ, u and p and $\psi\doteq\phi+p$ and **b** represents the direction of the magnetic field. The subscripts $\parallel$ and $\perp$ denote the components that are parallel to or perpendicular to the field line, respectively. Two of the dissipation parameters $\nu_\parallel$ and $\chi_\parallel$ primitively model the effect of the Landau damping and they are set to be of order one. Other parameters in Eqs. (1)–(3) are $\tau=T_i/T_e$, $\overline{K}=K-\Gamma$, $K=\eta_i+1$, where η_i is the measure of the ITG, and Γ is the adiabatic gas constant. The units of Eqs. (1)–(3) are the gyroradius ρ_s of the ion, with the electron temperature and the density-gradient length scale L_n for the space, perpendicular and parallel to the field line, respectively, L_n/v_s for the time, e/T_e for the electric potential, and ρ_s/L_n for the size of the perturbations. For the analysis, zero boundary conditions in the x direction and the periodic conditions in the y and z directions. The major point of Eqs. (1)–(3) is that they yield the level of the turbulence comparable to the simulation results of the more sophisticated kinetic models. This is the main reason that we choose Eqs. (1)–(3) as our model though they lack the simulated effect of the gyro-Landau damping. The same method, in principle, can be applied to the models of more complex nature without further conceptual complications.

In order to obtain the Euler-Lagrange equations we proceed to obtain the flux conservation by taking the averages of Eqs. (1)–(3) over the y and z directions. In the steady state, after the integration over x and upon using the zero boundary conditions, Eqs. (1)–(3) yield

$$\frac{d^2\langle\phi\rangle}{dx^2} = -\chi_\perp^{-1}\frac{\partial Q}{\partial x} + \mu_\perp^{-1}\Delta W(x), \tag{4}$$

$$\frac{d\langle u\rangle}{dx} = \nu_\perp^{-1}\Delta R(x), \tag{5}$$

$$\frac{d\langle p\rangle}{dx} = \chi_\perp^{-1}\Delta Q(x). \tag{6}$$

In the above, the heat flux Q and the Reynolds stresses R and W are defined as

$$Q \doteq -\left\langle p\frac{\partial\phi}{\partial y}\right\rangle, \quad R \doteq -\left\langle p\frac{\partial u}{\partial y}\right\rangle, \quad W \doteq -\left\langle \frac{\partial(\phi+p)}{\partial x}\frac{\partial\phi}{\partial y}\right\rangle \tag{7}$$

and $\Delta Q \doteq Q - \overline{Q}$, as the difference of the y-z average from the volume average. Equations (4)–(6) show the relations between the mean profiles and the fluxes of the fluctuations.

In this work, closure of the moments is achieved rigorously upon using the boundary conditions. First, we obtain the equations for the fluctuations by subtracting the averaged equations from Eqs. (1)–(3). Then, from them, one obtains the conservation law of energy $\mathcal{E}$,

$$\mathcal{E} \doteq \frac{1}{2}\left[\overline{|\widetilde{\phi}|^2} + \overline{|\nabla_\perp\widetilde{\psi}|^2} + \overline{|\widetilde{u}|^2} + \frac{1}{\Gamma\tau}\overline{|\widetilde{p}|^2}\right], \tag{8}$$

by multiplying by $\widetilde{\phi}$, $\widetilde{u}$, and $\widetilde{p}$, respectively, by integrating over x and by adding up,

$$\overline{Q} = \frac{\Gamma}{K}(\mathcal{N}+\mathcal{D}). \tag{9}$$

In Eq. (9), we define

$$\mathcal{N} = \frac{1}{\chi_\perp\Gamma\tau}\overline{|\Delta Q|^2} + \frac{1}{\mu_\perp}\overline{|\Delta W|^2} + \frac{1}{\nu_\perp}\overline{|\Delta R|^2}, \tag{10}$$

which is the fourth-order quantity in terms of the fluctuations and represents the energy-production rate due to the gradient of the mean profiles, and

$$\mathcal{D} = \mu_\perp\overline{|\nabla_\perp^2(\widetilde{\phi}+\widetilde{p})|^2} + \nu_\perp\overline{|\nabla_\perp\widetilde{u}|^2} + \nu_\parallel\overline{|\nabla_\parallel\widetilde{u}|^2} + \frac{\chi_\perp}{\Gamma\tau}\overline{|\nabla_\perp\widetilde{p}|^2} + \frac{\chi_\parallel}{\Gamma\tau}\overline{|\nabla_\parallel\widetilde{p}|^2}, \tag{11}$$

which denotes the loss of energy by various dissipations. Since the left-hand side of Eq. (9) is the second order and $\mathcal{N}$ is fourth order, it is obvious that the size of the fluctuations cannot be infinite and Q is of finite quantity.

The *naive* choice of the variational functional would be to maximize the heat flux under the condition of Eq. (9),

$$\mathcal{A}' = \overline{Q} + \lambda'\left[\overline{Q} - \frac{\Gamma}{K}(\mathcal{N}+\mathcal{D})\right], \tag{12}$$

where λ' is the undetermined Lagrange multiplier. The variational derivatives of typical terms in Eq. (12) are

$$\frac{\delta\overline{Q}}{\delta\widetilde{\phi}(\boldsymbol{x})} = \frac{\partial\widetilde{p}}{\partial y}, \quad \frac{\delta\overline{|\Delta Q|^2}}{\delta\widetilde{\phi}(\boldsymbol{x})} = 2\Delta Q(\boldsymbol{x})\frac{\partial\widetilde{p}}{\partial y} \tag{13}$$

and, thus, the corresponding Euler-Lagrange equation yields

$$\widetilde{u} = 0. \tag{14}$$

Since there is no motion along the field lines, the effect of magnetic shear does not exist and, thus, the eigenfunctions are not localized near the rational surface but spread all over the place and upper bound for the heat flux becomes unreasonably large.

In order to *improve* the shortcomings one must include other constraints that keep the important effects of the magentic shear intact. As one way of doing so, we pursue the following: Upon averaging Eq. (2) and using Eq. (5), we obtain another condition,

$$\overline{G} = \nu_\perp^{-1}\overline{|\Delta R|^2} + \nu_\perp\overline{|\nabla_\perp u|^2} + \nu_\parallel\overline{|\nabla_\parallel u|^2}, \tag{15}$$

where

$$G(x) \doteq -\langle u\nabla_\parallel(\phi+p)\rangle \tag{16}$$

expresses the energy supply to the parallel motion due to the electric field and the pressure gradient. Magnetic shear effects are apparent in G and the last term on the right-hand side of Eq. (15) as the gradient along the field lines. Now, the new variational principle is *maximize the heat flux that satisfies the conditions Eqs. (9) and (15).* The variational functional is

$$\mathcal{A} = \overline{Q} + \lambda_1\left[\overline{Q} - \frac{\Gamma}{K}(\mathcal{N}+\mathcal{D})\right] + \lambda_2\left(\overline{G} - \frac{1}{\nu_\perp}\overline{|\Delta R|^2} - \nu_\perp\overline{|\nabla_\perp u|^2} - \nu_\parallel\overline{|\nabla_\parallel u|^2}\right), \tag{17}$$

where the constants λ_1 and λ_2 are yet to be determined.

After the variational differentiations, the Euler-Lagrange equations follow as

$$0 = \mu_\perp\nabla_\perp^2\Psi + \nabla_\parallel u - \zeta\frac{\partial p}{\partial y} + (\chi_\perp\Gamma\tau)^{-1}\Delta Q\frac{\partial p}{\partial y} - \nu^{-1}\Delta R\frac{\partial u}{\partial y} + \mu_\perp^{-1}\Delta W\frac{\partial^2}{\partial x\partial y}(2\phi+p), \tag{18}$$

$$0 = \nu_\perp\nabla_\perp^2 u + \nu_\parallel\nabla_\parallel^2 u - \nabla_\parallel(\phi+p) + \nu_\perp^{-1}\Delta R\frac{\partial\phi}{\partial y}, \tag{19}$$

$$0 = \mu_\perp\nabla_\perp^2\Psi + \nabla_\parallel u + \zeta\frac{\partial\phi}{\partial y} - \frac{\chi_\perp}{\Gamma\tau}\nabla_\perp^2 p - \frac{\chi_\parallel}{\Gamma\tau}\nabla_\parallel^2 p - (\chi_\perp\Gamma\tau)^{-1}\Delta Q\frac{\partial\phi}{\partial y} + \mu_\perp^{-1}\Delta W\frac{\partial^2\phi}{\partial x\partial y}. \tag{20}$$

In Eqs. (18)–(20), the new shorthanded parameters are

$$\zeta \doteq \frac{K(1+\lambda_1)}{2\lambda_1 \Gamma},$$

$$\lambda_1 = \frac{K\overline{Q}}{\Gamma}\left[\frac{1}{\chi_\perp \Gamma \tau}\overline{|\Delta Q|^2} + \frac{1}{\mu_\perp}\overline{|\Delta W|^2} - \frac{1}{\nu_\perp}\overline{|\Delta R|^2}\right]^{-1},$$

$$\Psi \doteq \nabla_\perp^2(\phi + p), \tag{21}$$

where ζ and λ_1 are obtained after Eqs. (18)–(20) are multiplied by $\tilde{\phi}$, $\tilde{u}$, and $\tilde{p}$, correspondingly, and the volume averages are taken upon using Eqs. (9) and (15).

II. RESULTS AND DISCUSSION

The critical value η_{ic}, below which perturbations of arbitrary size vanish monotonically in time, is computed. It serves two purposes: Firstly, physically it is important to know the value of η_{ic} and the critical state; secondly, for a value of η_i that is slightly bigger than η_{ic}, one may use the critical profiles as initial input in the iterative scheme of the numerical procedure. The above mentioned η_{ic} is the value that determines the energy stability criterion and it is smaller than the often calculated value of the linear stability. The critical state is obtained from Eqs. (18)–(20) by setting the nonlinear terms to vanish, $\lambda_1 \to \infty$ and $\zeta \to K/2\Gamma$. The parallel gradient in the slab is $\nabla_\parallel = k_z + s k_y x$, where k_z is the differnce of the wave vector in the z (toroidal) direction to that of the mode-rational surface and x is the (radial) distance from the rational surface. The eigenvalue equations are, then, Fourier transformed in y and z and are solved by the shooting method varying the modes (k_y, k_z). Out of the many eigenvalues of ζ, the least value is chosen in computing the critical value η_{ic} and the corresponding mode number generates the critical state of the energy stability. After the critical state is identified, we proceed for higher values of η_i by iteratively computing the eigenfuctions starting from the critical profiles. As the solver, we use the routine DVCPR of the International Mathematics and Statics Library (IMSL), which can vary the mesh size with an error-correction mechanism.

The parameters used for the analysis are $\Gamma = 2$, $\tau = 1$, $s = 0.1$, $\chi_\parallel = \nu_\parallel = 1$ and the size of the plasma is $-40 \leqslant x \leqslant 40$, $0 \leqslant y \leqslant 10\pi$ and $0 \leqslant z \leqslant 7.5\pi$, which are the same as those in Ref. [16]. In the case of $\chi_\perp = \nu_\perp = \mu_\perp = 0.01$, $\eta_{ic} \approx -0.884$ and for the case of $\chi_\perp = \nu_\perp = \mu_\perp = 0.5$ $\eta_{ic} \approx -0.563$. For both cases, the critical mode is $(m,n) = (1,0)$, which means that the mode number along z is the same as that of the mode-rational surface. These values are much smaller than both the typical experimental values and the critical value of the linear stability, which are of order 1. This is not surprising because of the more stringent requirement of the energy stability than the linear stability.

For the values of η_i that are larger than η_{ic}, the nonlinear terms in Eqs. (18)–(20) are no longer negligible and, thus, many other modes contribute to the evolution of one mode through the mode couplings of the nonlinear interactions. However, in the present work, we keep only one eigenmode $(m,n) = (1,0)$. The reason is more practical than anything else—even for this case, much computer memory and time is needed. Hence, one may argue that our result is only acceptible for the η_i's close to η_{ic}. Yet, with this limitation in mind, one can still estimate reasonably, after the extrapolation of the present calculation, by realizing that, in earlier works of similar nature in the fluids, single-mode study provides a certain fruitful result. Before we move on, we would like to make a remark on Eqs. (18)–(20). Since ϕ and p are even in x and u is odd, Q is even and R and W are odd. These symmetries lead to $R = W = 0$ and to the observation that $\langle p \rangle$ is odd, being positive for $x > 0$ and negative for $x < 0$ from Eq. (6). This is good because, if the equilibrium pressure is higher to the left of the rational surface, turbulence operates in such a way as to reduce the pressure gradient. Figure 1 shows the bounding curve of the volume-averaged heat flux versus η_i for the cases of $\chi_\perp = 0.5$ and $\chi_\perp = 0.01$. As the value of η_i increases beyond η_{ic}, it becomes more and more difficult to have the convergent solution because of the formation of the boundary layer. It is to be noted that the volume averages are taken over part of the volume where the heat flux is appreciable, that is 50% (in the case of $\chi_\perp = 0.5$) or 20% (in the case of $\chi_\perp = 0.01$) of the box size. For η_i about 0.13 higher than the critical value

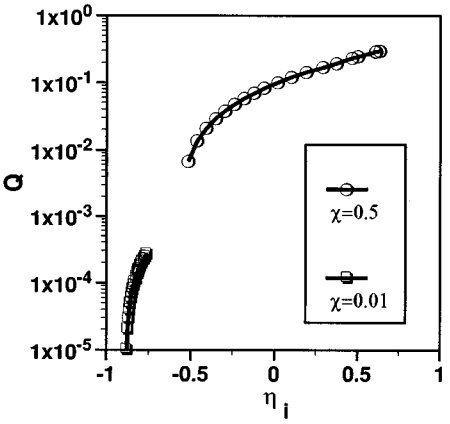

FIG. 1. Bounding curve of the upper bound for the heat flux and η_i. Squares are for the case of $\chi_\perp = 0.01$ and the circles for $\chi_\perp = 0.5$. The unit of the heat flux is $(\rho_s / L_n^2)(cT_e/eB)$ normalized to pressure.

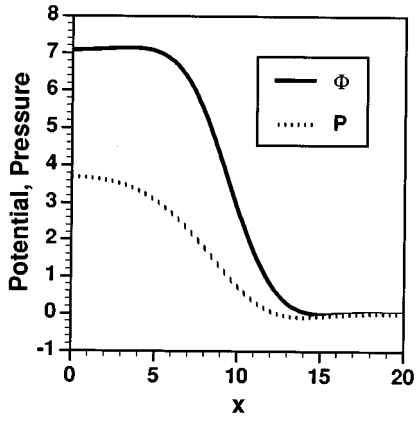

FIG. 2. Typical profiles of the fluctuations of the potential (solid curve) and the pressure (dotted curve).

when $\chi_\perp = 0.01$, the upper bound is about $3\times10^{-4}(\rho_s/L_n^2)\times(cT_e/eB)$ normalized in terms of the center pressure. As a reference for the case when $\eta_i = 2$, the direct numerical simulation reports that the volume-averaged heat flux $Q \approx 1$ [16]. Although, at present, η_i is far from the experimental value and comparing the upper bound to the real transport is seemingly unrealistic, one can conclude positively, in a limited fashion, that the upper bound would not be far off the true value as the calculation of larger $\chi_\perp$ indicates. In Fig. 2, typical eigenfunctions of the potential and the pressure are plotted.

Extension of the present work is possible with better numerical algorithms and the application of the present formalism to models of a more complex nature, either fluid or kinetic, is left to a future work. Lower bound for the heat transport may also be interesting and the work is in progress.

ACKNOWLEDGMENTS

The author is grateful to Dr. J. A. Krommes for critical discussions. Numerical computation by Ms. Kang-Oak Choi is pleasantly acknowledged. This work is supported by the Korea Science and Engineering Foundation (KOSEF) Grant No. 931-0200-034-2 and by the Korean Ministry of Education Grant No. BSRI-96-2456.

[1] B. Coppi and F. Pegoraro, Nucl. Fusion **17**, 969 (1977).
[2] B. Coppi, M. N. Rosenbluth, and R. Z. Sagdeev, Phys. Fluids **10**, 582 (1967).
[3] W. Horton, D. I. Choi, and W. M. Tang, Phys. Fluids **24**, 1077 (1981).
[4] S. M. Wolfe, M. Greenwald, R. Gandy, R. Granetz, C. Gomez, D. Gwinn, B. Lipschultz, S. McCool, E. Marmat, J. Parker, R. R. Parker, and J. Rice, Nucl. Fusion **26**, 329 (1986).
[5] F. X. Soeldner, E. R. Muller, F. Wagner, H. S. Bosch, A. Eberhagen, H. U. Fahrbach, G. Fussmann, O. Gehre, K. Gentle, J. Gernhardt, O. Gruber, W. Herrmann, G. Janeschitz, M. Kornherr, K. Krieger, H. M. Mayer, K. McCOrmick, H. D. Murmann, J. Neuhauser, R. Nolte, W. Poschenrieder, H. Roehr, K.-H. Steuer, U. Stroth, N. Tsois, and H. Verbeek, Phys. Rev. Lett. **61**, 1105 (1986).
[6] S. D. Scott, P. H. Diamond, R. J. Fonck, R. J. Goldston, R. B. Howell, K. P. Jaenig, G. Schilling, E. J. Synakowski, M. C. Zarnstorff, C. E. Bush, E. Fredrickson, K. W. Hill, A. C. Janos, D. K. Mansfield, D. K. Owens, H. Park, G. Pautasso, A. T. Ramsey, J. Schivell, G. D. Tait, W. M. Tang, and G. Taylor, Phys. Rev. Lett. **64**, 531 (1990).
[7] S. Hamaguchi and W. Horton, Phys. Fluids B **2**, 1833 (1990).
[8] S. E. Parker, W. Dorland, R. A. Santoro, M. A. Beer, Q. P. Liu, W. W. Lee, and G. W. Hammett, Phys. Plasmas **1**, 1461 (1994).
[9] G. W. Hammett and F. W. Perkins, Phys. Rev. Lett. **64**, 3019 (1990).
[10] W. Dorland and G. W. Hammett, Phys. Fluids B **5**, 812 (1993).
[11] L. N. Howard, J. Fluid Mech. **17**, 405 (1963).
[12] F. H. Busse, Adv. Appl. Mech. **18**, 77 (1978).
[13] J. A. Krommes and R. A. Smith, Ann. Phys. (N.Y.) **177**, 246 (1987).
[14] C.-B. Kim and J. A. Krommes, Phys. Rev. A **42**, 7487 (1990).
[15] C. Y. Wang and A. Bhattacharjee, Phys. Fluids B **3**, 3462 (1991).
[16] C.-B. Kim, W. Horton, and S. Hamaguchi, Phys. Fluids B **5**, 1516 (1993).